DOI: 10.1002/chem.200801238

VIP

Fluorescence Emission from 2,6-Naphthylene-Bridged Mesoporous Organosilicas with an Amorphous or Crystal-Like Framework

Norihiro Mizoshita,[a, b] Yasutomo Goto,[a, b] Mahendra P. Kapoor,[a, c] Toyoshi Shimada,[b, d] Takao Tani,[a, b] and Shinji Inagaki*[a, b]

Abstract: We report that 2,6-naphthylene-bridged periodic mesoporous organosilicas exhibit unique fluorescence behavior that reflects molecular-scale periodicities in the framework. Periodic mesoporous organosilicas consisting of naphthalene–silica hybrid frameworks were synthesized by hydrolysis and condensation of a naphthalene-derived organosilane precursor in the presence of a template surfactant. The morphologies and meso- and molecular-scale periodicities of the organosilica materials strongly depend on the synthetic conditions. The naphthalene moieties embedded within the molecularly ordered framework exhibited a monomer-band emission, whereas those embedded within the amorphous framework showed a broad emission attributed to an excimer band. These results suggest that the naphthalene moieties fixed within the crystal-like framework are isolated in spite of their densely packed structure, different from conventional organosilica frameworks in which only excimer emission was observed for both the crystal-like and amorphous frameworks at room temperature. This key finding suggests a potential to control interactions between organic groups and thus the optical properties of inorganic/organic hybrids.

Keywords: fluorescence · hybrid materials · mesoporous materials · organosilicates · self-assembly

Introduction

Inorganic/organic hybrid materials are promising as next-generation functional materials because various functionalities of inorganic and organic species are available, compatible, and cooperative in the design of such materials.[1] To introduce enhanced properties, the control of inorganic/organic hybrid structures on various scales of length is of great importance as reported in recent reviews.[1] Organic-functionalized mesoporous silicas, which are synthesized by post-synthesis grafting of mesoporous silicas or direct condensation of organosilane precursors in the presence of template surfactants, are hierarchically structured inorganic/organic hybrids that have the potential for various applications, such as adsorbents, optical devices, sensors, catalysts, mass and ion conductors, and biomimetic systems.[2,3]

In particular, periodic mesoporous organosilicas (PMOs) synthesized by using bridged organosilane precursors $(R'O)_3Si\text{-}R\text{-}Si(OR')_3$ are a new class of inorganic/organic hybrid material in which the organic bridging groups (-R-) are densely and covalently embedded within the silica frameworks.[4–7] Moreover, our group achieved the induction of molecular-scale periodicity in the organosilica frameworks, that is, crystal-like ordering of pore walls for 1,4-phenylene- and 4,4′-biphenylylene-bridged PMOs by applying basic hydrolytic conditions.[8–10] The formation of molecular-scale ordering is advantageous for high functionalization of the framework of PMOs by adjusting the interactions between the organic groups.[8–15] To control these interactions, it is necessary to understand the effects of molecular-

[a] Dr. N. Mizoshita, Dr. Y. Goto, Dr. M. P. Kapoor, Dr. T. Tani, Dr. S. Inagaki
Toyota Central R&D Laboratories, Inc.
Nagakute, Aichi 480–1192 (Japan)
Fax: (+81) 561-63-6507
E-mail: inagaki@mosk.tytlabs.co.jp

[b] Dr. N. Mizoshita, Dr. Y. Goto, Prof. Dr. T. Shimada, Dr. T. Tani, Dr. S. Inagaki
Core Research for Evolutional Science and Technology (CREST)
Japan Science and Technology Agency (JST)
Kawaguchi, Saitama 332–0012 (Japan)

[c] Dr. M. P. Kapoor
Present address: Taiyo Kagaku Co., Ltd.
1–3 Takaramachi, Yokkaichi
Mie 510–0844 (Japan)

[d] Prof. Dr. T. Shimada
Department of Chemical Engineering
Nara National College of Technology
Yamatokoriyama, Nara 639–1080 (Japan)

Supporting information for this article is available on the WWW under http://dx.doi.org/10.1002/chem.200801238.

scale ordering on the chemical and physical properties of the organic moieties embedded within the frameworks, although there have not been any reports on this issue.[16–21] In addition, it is also important to expand the number of organic groups to form crystal-like ordering of pore walls for the development of further functionalized PMOs.

Our intention herein is to introduce a 2,6-naphthylene bridging group into frameworks of PMOs (Scheme 1). Naphthalene-based organosilicas are expected to form mesoporous structures with crystal-like pore walls because of the rigidity and planarity of the naphthalene ring. Naphthalene moieties are also available as a fluorescence probe to examine the local environments of the organic bridging groups. In contrast to 1,4-phenylene and 4,4′-biphenylylene bridging groups, because two Si–C bonds of the 2,6-naphthylene bridge are not in a straight line, the rotational motion of the naphthalene ring around the Si–C bond axis can be restricted after sufficient condensation of the siloxane networks (Scheme 1). Recently, we reported the fluorescence behavior of PMO thin films containing various aromatic bridging groups, which were prepared by spin-coating with solutions of acidic ethanol sol at room temperature (the so-called evaporation-induced self-assembly method).[21] However, the sol–gel PMO films had amorphous pore walls, that is, no definite periodic structure within the organosilica frameworks.

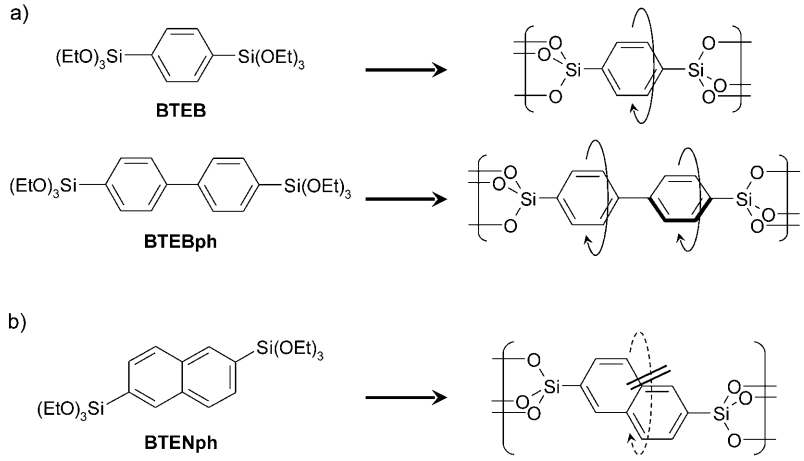

Scheme 1. Chemical structures of organosilane precursors with aromatic bridging groups and a schematic illustration of the plausible rotational motions of the bridging groups in organosilica hybrid frameworks: a) 1,4-phenylene and 4,4′-biphenylylene bridges, b) 2,6-naphthylene bridge.

Herein, we report the structures and fluorescence properties of 2,6-naphthylene-bridged PMO powders synthesized by hydrolysis and condensation of the naphthalene-based precursor 2,6-bis(triethoxysilyl)naphthalene (BTENph; Scheme 1) in aqueous solutions containing a cationic surfactant (i.e., octadecyltrimethylammonium chloride (C_{18}TMACl)) as a structure-directing agent. Various acidic and basic hydrolytic conditions were selected to control the meso- and molecular-scale periodic structures. Naphthalene-based PMOs with crystal-like pore walls were successfully obtained under an optimized basic reaction condition. Fluorescence behavior was examined for 2,6-naphthylene- and 4,4′-biphenylylene-bridged PMOs. A fluorescence study showed that 2,6-naphthylene groups fixed within the crystal-like framework are isolated without interacting with one another, whereas those in an amorphous framework are likely to form associated species.

Results and Discussion

Preparation of mesoporous naphthalene–silica hybrids: The acidic and basic reaction conditions under which the 2,6-naphthylene-bridged organosilica powders were prepared are given in Table 1 and Table 2, respectively. Naphthalene-based organosilica materials were obtained as white powders (**A1**–**A4** and **B1**–**B6**). Figure 1 shows the X-ray diffraction (XRD) patterns of **A1**, **B1**, **B2**, and **B4**.

The acid-catalyzed synthesis of naphthalene–silica powders resulted in mesoporous materials made of amorphous naphthalene–silica frameworks. In the XRD pattern of **A1**, a single broad peak was observed at $d = 4.49$ nm (as synthesized), which indicates the formation of periodic mesoporous channels and amorphous pore walls consisting of a naphthalene–silica hybrid (Figure 1a). Similar XRD patterns were obtained for naphthalene–silica materials **A2**–**A4**. The meso-scale periodicity of **A2**–**A4** ($d =$ 4.49–4.70 nm) is close to that of **A1** regardless of the BTENph/C_{18}TMACl ratios and the reaction conditions (Table 1).

Table 1. Synthesis of naphthalene–silica hybrids under acidic conditions.

Sample	HCl aq. [M]	Reaction conditions reaction temperature	Structure of organosilica[a] meso-scale periodicity	molecular-scale periodicity
A1[b]	0.86	RT (24 h), 95 °C (24 h)	○	–
A2[c]	0.86	RT (24 h), 95 °C (24 h)	○	–
A3[b]	0.86	90 °C (48 h)	○	–
A4[d]	0.67	RT (24 h), 95 °C (24 h)	○	–

[a] ○: formation of meso- or molecular-scale periodicity. [b] BTENph/C_{18}TMACl = 3:4 (w/w). [c] BTENph/C_{18}TMACl = 3:8. [d] BTENph/C_{18}TMACl = 1:1.

For organosilica materials obtained from basic reaction mixtures, slight changes in the reaction conditions signifi-

Table 2. Synthesis of naphthalene–silica hybrids under basic conditions

Sample	Reaction conditions		Structure of organosilica[a]	
	NaOH aq. [M]	reaction temperature	meso-scale periodicity	molecular-scale periodicity
B1	0.06	RT (24 h), 95 °C (24 h)	–	○
B2	0.06	RT (72 h)	○	–
B3	0.24	RT (24 h), 95 °C (24 h)	–[b]	○
B4	0.24	RT (48 h), 60 °C (24 h), 95 °C (24 h)	○	○
B5	0.24	95 °C (48 h)	–	○
B6	0.24	RT (48 h)	○	–
B7	0.55	RT (24 h), 95 °C (24 h)	–[c]	–[c]

[a] ○: formation of meso- or molecular-scale periodicity. [b] Broad diffraction at $2\theta \approx 1.9°$ was observed in the XRD pattern (see the Supporting Information). [c] No precipitation was formed.

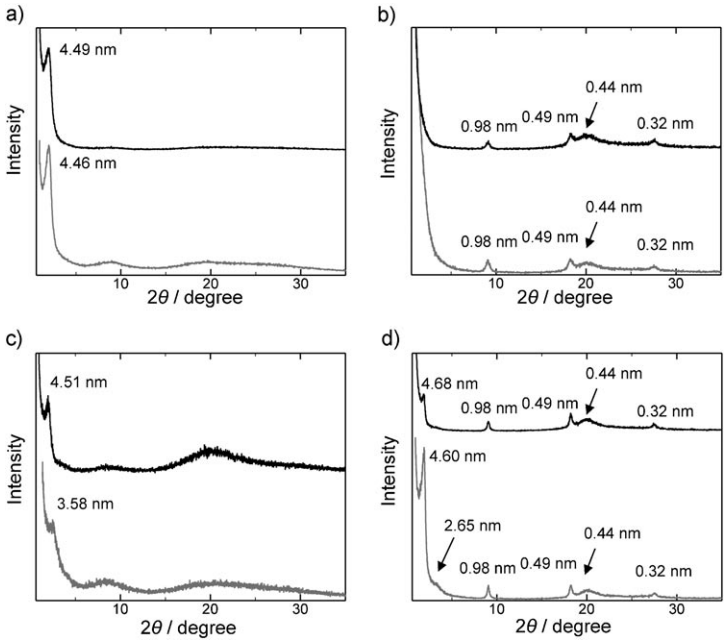

Figure 1. XRD patterns of a) **A1**, b) **B1**, c) **B2**, and d) **B4**. Black: as-synthesized sample; gray: extracted sample.

cantly influenced the meso- and molecular-scale periodic structures of the resultant naphthalene–silica hybrids (Table 2). For organosilica material **B1** prepared in a 0.06 M NaOH aqueous solution with thermal treatment at 95 °C, the XRD pattern showed sharp peaks at $d = 0.98$, 0.49, and 0.32 nm and a broad peak at $d = 0.44$ nm, without meso-scale periodicity. The three sharp peaks with the d-spacing ratio of 1:1/2:1/3 suggest the formation of a molecular-scale lamellar structure of the naphthalene–silica hybrid (Figure 1b). The interlayer spacing observed in the XRD measurements is in good agreement with that estimated from the layered model of 2,6-naphthylene-bridged silica (see Figure S1 in the Supporting Information). When a naphthalene–silica hybrid was prepared in a 0.06 M NaOH aqueous solution without thermal treatment, the resultant material (i.e., **B2**) showed only meso-scale periodicity (Figure 1c). These results indicate that the complexation of BTENph with the micellar aggregates of C_{18}TMACl occurred at low temperatures, but the thermal treatment resulted in the collapse of the meso-scale periodic structures and induction of the molecular-scale layer ordering of the frameworks (Figure 1b). Although molecular-scale periodicity is not induced in **B2**, broad diffractions at $2\theta \approx 9°$ in Figure 1c suggest that the precursory structure of the molecular-scale layer ordering is formed in the organosilica framework.[22] The extraction of the surfactant from **B2** led to partial collapse of the mesostructure as shown by the peak broadening and the decrease in the d-spacing (Figure 1c), thus indicating that the framework of **B2** is fragile. The synthesis of naphthalene–silica hybrids under more basic solutions was carried out because robust framework formation as a result of siloxane cross-links is necessary to obtain PMOs with crystal-like pore walls.

For **B3** prepared in a 0.24 M NaOH solution, the XRD pattern exhibited a broad diffraction in a small-angle region ($d \approx 4.6$ nm) in addition to four diffraction peaks in a wide-angle region, thus indicating that the partial arrangement of mesochannels with crystal-like pore walls is induced by increasing the NaOH concentration. A naphthalene–silica hybrid with both meso- and molecular-scale periodicities was successfully obtained for **B4** by applying longer reaction times at low temperatures (Table 2). The XRD pattern of **B4** showed a sharp diffraction peak at $d = 4.68$ nm (as synthesized), thus indicating the formation of periodic mesochannels, and four peaks corresponding to a molecular-scale periodic structure (Figure 1d). For extracted **B4**, a ratio of the reciprocal of two d-spacing values in a small-angle region ($d = 4.60$ and 2.65 nm) is $1:\sqrt{3}$, which implies the formation of a two-dimensional mesochannel array close to hexagonal packing.

The effects of the reaction temperature and NaOH concentration on the formation of meso- and molecular-scale periodicities were further examined for samples **B5**–**B7** (Table 2). In 0.24 M NaOH solutions, naphthalene-based PMOs with both meso- and molecular-scale periodicities were not obtained by stirring at either room temperature or 95 °C (**B5** and **B6**). In the case of sample **B7** with a 0.55 M NaOH solution as the reaction medium, no organosilica precipitate was formed. In the reaction mixture, a hydrolyzed silanol species of BTENph was stabilized because of an increased pH value, thus hindering the precursor from converting into siloxane species.

Morphologies of the PMOs **A1** and **B4** were observed by scanning electron microscopy (SEM) and transmission electron microscopy (TEM). The SEM image of **A1**, which consists of an amorphous organosilica framework, shows micrometer-scale aggregates with irregular shape (Figure 2a). On the other hand, naphthalene–silica **B4** with crystal-like pore walls exhibits a uniform rod-shaped morphology with lengths of 200–400 nm and widths of 70–80 nm (Figure 2b). Meso- and molecular-scale ordering shown by XRD measurements should be reflected in the submicrometer-scale particle morphology of **B4**. The TEM observation of **B4** fur-

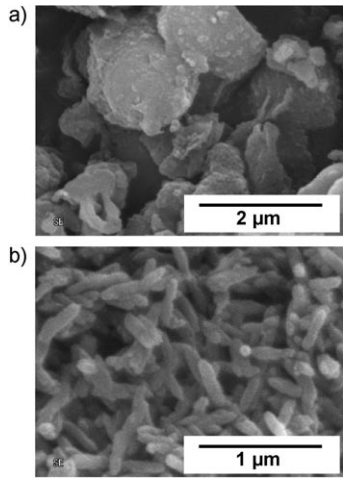

Figure 2. SEM images of a) **A1** and b) **B4** (extracted samples).

ther confirmed the meso- and molecular-scale periodic structures (Figure 3). The mesochannel array running along a long axis of the rod-shaped particle was observed (Figure 3a). The periodicity of the mesochannels is approxi-

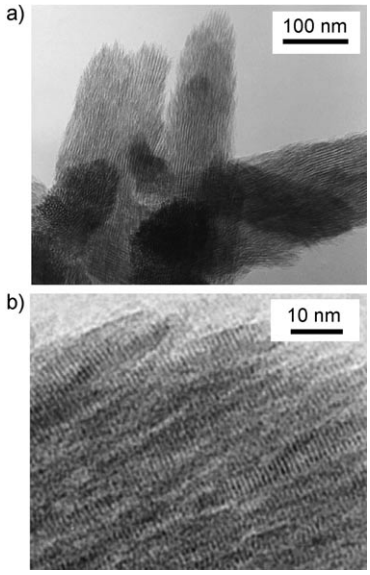

Figure 3. TEM images of naphthalene–silica hybrid **B4**.

mately 4–5 nm, which is in agreement with the XRD results. Moreover, molecular-scale periodicity was seen in the pore wall (Figure 3b). The fringe structure with a periodicity of approximately 1 nm corresponds to the 0.98-nm-layer ordering of the naphthalene–silica framework (Figure 1d). The molecular-scale lamellar structure is formed perpendicularly to the running direction of the mesochannels, which is similar to those reported for phenylene- and biphenylylene-bridged PMOs with molecular-scale periodicities.[8,9]

The porosity of the naphthalene-based mesoporous materials (extracted) was examined by nitrogen adsorption/desorption isotherm measurements (Figure 4). Organosilica materials **A1** and **B4**, for which the arrangement of the mesochannels was confirmed by XRD measurements, exhibited

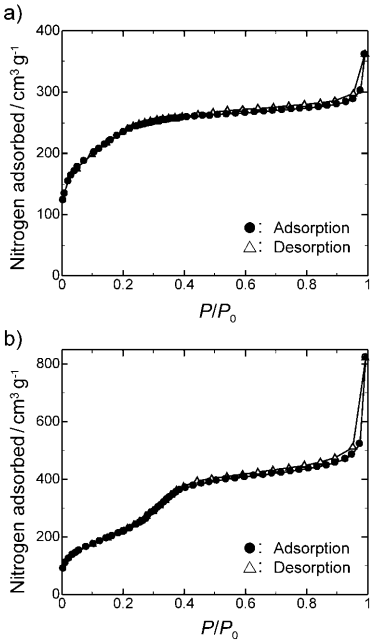

Figure 4. Nitrogen adsorption/desorption isotherms of a) **A1** and b) **B4** (extracted samples).

type IV nitrogen adsorption/desorption isotherms that are typical of periodic mesoporous materials. The Brunauer–Emmett–Teller (BET) surface area, pore diameter, and pore volume of **A1** are 847 $m^2 g^{-1}$, 2.58 nm, and 0.37 $cm^3 g^{-1}$, respectively, whereas for **B4**, these values are 807 $m^2 g^{-1}$, 3.66 nm, and 0.51 $cm^3 g^{-1}$, respectively. Considering the meso-scale periodicities observed by XRD measurements and the pore diameters, the amorphous pore wall of **A1** tends to be thicker than the densely packed crystal-like wall of **B4**. It is reasonable that the pore walls become thinner under the alkaline condition because of the strong ionic interaction between the surfactant cations and silicate anions.

The ^{29}Si magic-angle spinning (MAS) NMR spectra of the naphthalene–silica hybrids were measured to examine the degree of condensation of the ethoxysilyl groups of BTENph (Figure 5). Organosilica materials **A1** and **B2** with amorphous walls consist of partially hydrolyzed siloxane networks rich in T^2 ($R{-}Si(OH)(OSi)_2$) species. On the other hand, molecularly-ordered organosilica hybrids **B1** and **B4** contain both T^2 and fully condensed T^3 ($R{-}Si(OSi)_3$) species regardless of the formation of the periodic mesochannels. The peak intensity of the T^3 species of **B4** at $\delta = -82.1$ ppm is comparable to that of the T^2 species at $\delta = -71.3$ ppm. These results show that naphthalene–silica hybrids with crystal-like frameworks, which were synthesized under basic conditions, consist of well-condensed siloxane networks. The absence of Q species ($Si(OH)_{4-n}(OSi)_n$) in the NMR spectra

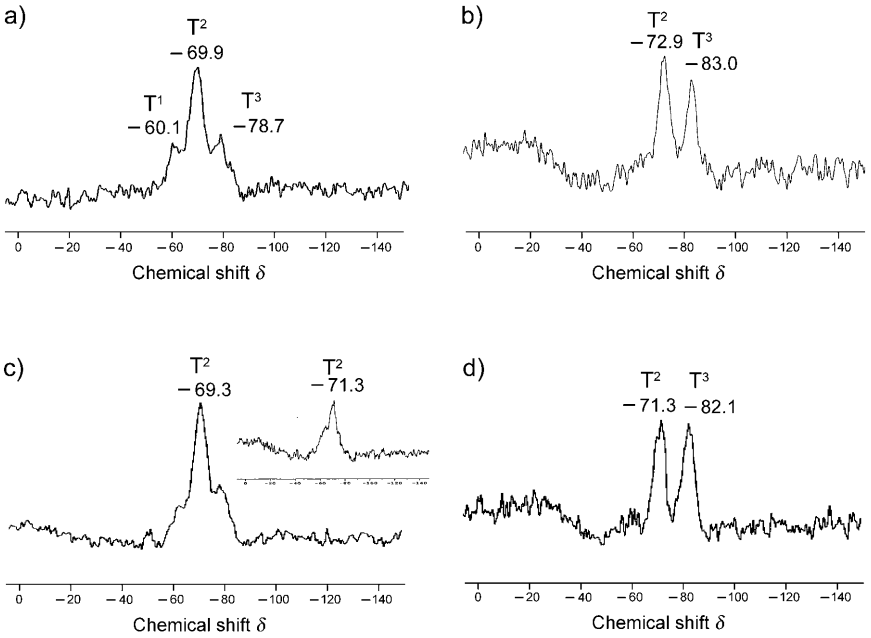

Figure 5. ^{29}Si MAS NMR spectra of a) **A1**, b) **B1**, c) **B2**, and d) **B4** (extracted samples). Inset of (c) shows the spectrum of as-synthesized **B2**.

indicates no cleavage of the Si–C bonds of BTENph during the syntheses of naphthalene–silica.

For the formation of naphthalene-based PMOs with crystal-like frameworks, reaction conditions that can induce the following two processes are required: 1) Complexation of surfactants and hydrolyzed precursors that form siloxane networks under mild hydrolytic conditions (formation of mesostructures); 2) further condensation that forms organosilica frameworks rich in T^3 species under strong hydrolytic conditions (crystallization and stabilization of silica walls without losing meso-scale periodicity). The relationship between the reaction conditions and resultant hybrid structures is schematically illustrated in Figure 6.[23] The conversion from amorphous into crystal-like pore walls in phenylene-bridged PMOs was also observed by post-synthetic treatment with an alkaline solution.[24]

Fluorescence study of mesostructured organosilica hybrids with aromatic bridges: The fluorescence spectra of naphthalene-based PMOs **A1** and **B4** (as-synthesized) were measured to examine the local environments of the 2,6-naphthylene bridging groups incorporated into amorphous and crystal-like organosilica frameworks. We also compared their fluorescence behavior with that of the previously reported 4,4′-biphenylylene-bridged PMOs.[9,25] Figure 7a–c shows the fluorescence spectra of BTENph (in a solution of 2-propanol) and the naphthalene-based PMOs at room temperature (solid lines) upon excitation at $\lambda = 280$ nm. Naphthalene–silica **A1** with amorphous pore walls exhibited a broad emission band at $\lambda = 410$ nm attributed to excimer species of naphthalene moieties,[26] thus suggesting that the loose and irregular siloxane networks are likely to facilitate the formation of dimers or more associated species of naphthalene rings in the amorphous framework. Similar emission behavior was observed for naphthalene-based PMO films with amorphous frameworks.[21] In contrast, the emission wavelength of naphthalene–silica **B4** with crystal-like pore walls was $\lambda = 358$ nm because of monomeric species of naphthalene.[26] This result indicates that naphthalene moieties embedded within the crystal-like framework are isolated without forming associated species. Fluorescence quantum yields of **A1** and **B4** upon excitation at $\lambda = 280$ nm were 0.10 ± 0.01 and 0.15 ± 0.01, respectively. The higher quantum yield of **B4** suggests the decrease in quenching processes by the isolation of naphthalene moieties in the crystal-like framework.

The difference in the fluorescence behavior between amorphous and crystal-like naphthalene–silica frameworks

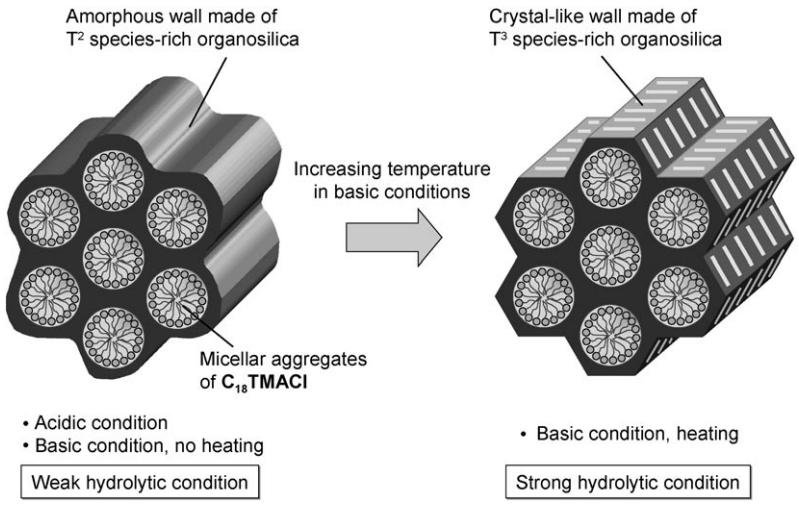

Figure 6. Schematic illustration of the formation of meso- and molecular-scale periodicities under various reaction conditions.

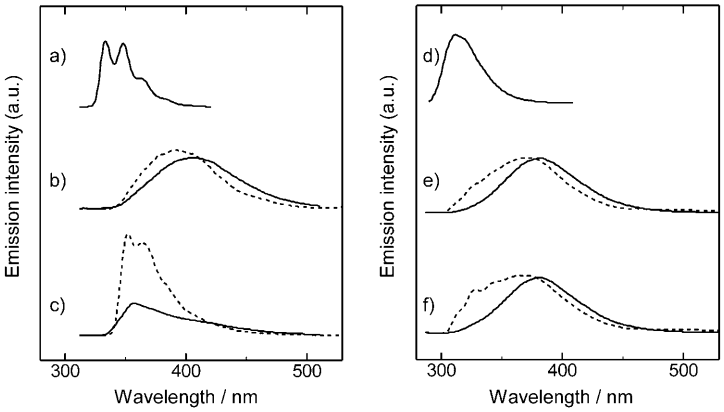

Figure 7. Fluorescence spectra of naphthalene- (left) and biphenyl-based PMOs (right) upon excitation at $\lambda = 280$ nm. a) Solution of BTENph in 2-propanol, b) as-synthesized **A1**, c) as-synthesized **B4**, d) a solution of BTEBph in 2-propanol, e) biphenyl-based PMO with amorphous wall, and f) biphenyl-based PMO with crystal-like wall. Solid line: fluorescence spectra obtained at room temperature; broken line: fluorescence spectra obtained at −196 °C.

became conspicuous at the temperature of liquid nitrogen (−196 °C), at which thermal fluctuations, such as rotational and vibrational motions, of the organosilica frameworks are restricted (Figure 7b,c, broken lines). The emission band of **A1** showed a slight blue shift by cooling from room temperature to −196 °C. The broad emission spectrum, however, still suggests the formation of excimer species, although it may be slightly restricted at −196 °C. On the other hand, for organosilica **B4**, a distinct monomer band emission with vibronic structures was observed at −196 °C, accompanied by the obvious increase of the emission intensity. The spectral shape is similar to that of the dilute solution of BTENph (Figure 7a). This behavior indicates that the isolation of the naphthalene rings in the crystal-like framework becomes more remarkable at −196 °C by suppressing the molecular motions.

The distinct monomer-band emission of naphthalene–silica **B4** also presented a striking contrast to the fluorescence behavior of the biphenyl-based PMOs (Figure 7d–f). The biphenyl–silica PMOs exhibited excimer band emissions at room temperature for both the amorphous and crystal-like pore-wall structures (Figure 7e,f, solid lines), thus indicating that the 4,4′-biphenylylene bridges embedded within the amorphous and the crystal-like frameworks are interactive with one another. The fluorescence quantum yield of the biphenyl-based PMO with the crystal-like framework (i.e., 0.38 ± 0.04, excited at $\lambda = 266$ nm) was also similar to that of the PMO with the amorphous biphenyl–silica framework (i.e., 0.38 ± 0.04, excited at $\lambda = 266$ nm), thus suggesting a resemblance of interactions between neighboring biphenyl moieties at room temperature.

The optical behavior of the naphthylene and biphenylylene bridging groups is quite different in the crystal-like organosilica frameworks, although they have similar lamellar packing structures as suggested by the XRD patterns.[9] The reason is not clear now, but would result from the restriction of rotational motion of the 2,6-naphthylene bridges in contrast to the 4,4′-biphenylylene bridges (Scheme 1). When the fluorescence spectra of the biphenyl—silica species were measured at −196 °C (Figure 7e,f, broken lines), the excimer band emissions showed blue shifts similar to **A1**. For the biphenyl–silica species with the crystal-like framework, a slight enhancement of the emission intensity around $\lambda =$ 320 nm was observed (Figure 7f) in comparison with the biphenyl-based PMO with amorphous walls (Figure 7e). Because the emission band at $\lambda = 320$ nm is probably a result of monomeric species of the biphenyl moiety (Figure 7d), the fluorescence behavior indicates that partial isolation of the organic moieties can occur in the 4,4′-biphenylylene-bridged crystal-like framework. Restriction of the rotational motions of the biphenyl moieties by cooling to −196 °C may result in the monomeric component in the fluorescence spectrum, although partial rotational motion of biphenyl species may still be allowed in comparison with 2,6-naphthylene bridges. A remarkable increase in the emission intensity by cooling to −196 °C is observed only for the naphthalene–silica **B4** that exhibits monomer band emission (Figure 7). For the other three organosilica hybrids, excimer band emissions are still dominant. Because associated chromophores are normally less emissive than monomeric species, the emission behavior of **B4** with the naphthylene bridges isolated in the framework suggests one potential approach to improving the emission intensity of inorganic/organic hybrid materials containing large amounts of organic chromophores.

Molecular modeling of organosilica clusters supports that 2,6-naphthylene bridging groups in crystal-like organosilica frameworks are monomeric, whereas those in amorphous structures tend to form associated species (see Figure S4 in the Supporting Information). In the amorphous networks consisting of T^2-type siloxane cross-links, naphthalene rings can partly form dimers in the ground state. The dynamic motion of the loosely cross-linked frameworks also seems to allow the naphthalene rings to form associated species in the excited states. In the crystal-like structure, three-dimensional rigid siloxane networks based on the T^3-type cross-links fix the spatial arrangement of the naphthalene rings in their lateral directions with intervals of 0.42–0.46 nm, which are longer than typical π–stacking distances (i.e., ≈0.35 nm), thus inhibiting interaction between the naphthalene rings.

Conclusion

In the present study, 2,6-naphthylene-bridged mesoporous organosilica hybrids were prepared under acidic and basic reaction conditions. Optimization of the basic hydrolytic conditions led to the formation of mesoporous naphthalene–silica hybrids with molecular-scale periodicity in the framework. In the crystal-like framework, the 2,6-naphthylene bridging groups exhibited sharp emission spectra attributed to a monomer band, whereas excimer band emissions were observed for amorphous organosilica hybrids. These results

suggest that the naphthalene moieties fixed within the crystal-like framework are isolated in spite of their densely packed structure, different from conventional biphenyl–silica frameworks in which only the emission of the excimer band was observed for both of crystal-like and amorphous frameworks at room temperature. This unique finding suggests that the interactions, and thus the optical properties, of the organic moieties embedded within the organosilica frameworks are controllable by arranging the inorganic/organic hybrid structures and brings about a progress of optical applications of organosilica hybrid materials.

Experimental Section

General: All reagents and solvents were of the highest commercial quality and were used without further purification. The cationic surfactant C_{18}TMACl was purchased from TCI. The naphthalene-based precursor BTENph was synthesized by the Rh-catalyzed silylation of 2,6-dibromonaphthalene, as reported previously,[21,27] and obtained in an improved yield. The ^{1}H and ^{13}C NMR spectra were measured on a JEOL JNM-LA500 spectrometer. High-resolution mass spectroscopy (HRMS) was performed on a JEOL JMS-700 spectrometer. Fluorescence spectra were obtained on a JASCO FP-6500 spectrometer. Fluorescence quantum yields were determined by using a photoluminescence quantum yield measurement system equipped with a calibrated integrating sphere (Hamamatsu Photonics C9920–02). IR measurements were conducted on a Thermo Nicolet Avatar 360 FT-IR spectrometer with an attenuation total reflection (ATR) attachment.

Characterization of meso-structured materials: XRD measurements were performed on a Rigaku RINT-TTR diffractometer with $Cu_{K\alpha}$ radiation (50 kV, 300 mA). SEM observations were conducted on a Hitachi S-3600N with an accelerating voltage of 15 kV for samples coated with gold. TEM observations were performed on a JEOL EX2000 machine with an accelerating voltage of 200 kV. Nitrogen adsorption/desorption isotherms were measured on a Quantachrome Autosorb-1 sorptometer at −196 °C. Prior to the measurements, all the samples were outgassed at 110 °C. BET surface areas were calculated from the linear section of the BET plot ($P/P_0 = 0.05$–0.2). Pore-size distributions were determined by using the density functional theory (DFT) method (the DFT kernel: N_2 at 77 K on silica, cylindrical pore, nonlinear density functional theory (NLDFT) equilibrium model). Pore volumes were estimated by the *t*-plot method. The ^{29}Si MAS NMR spectra were recorded on a Bruker Avance 400 spectrometer at 79.49 MHz with 4-mm zirconia rotors and a sample spinning frequency of 5 kHz. The chemical shifts for all spectra were referenced to tetramethylsilane (TMS) at $\delta = 0$ ppm.

Synthesis of naphthalene-derived precursor BTENph: A mixture of 2,6-dibromonaphthalene (3.00 g, 10.49 mmol), $[Rh(CH_3CN)_2(cod)]BF_4$ (178 mg, 0.53 mmol: cod = cycloocta-1,5-diene), tetrabutylammonium iodide (7.80 g, 21.12 mmol), dimethylformamide (50 mL), and triethylamine (8.80 mL) was cooled to 0 °C. Triethoxysilane (7.70 mL, 42.00 mmol) was added to the reaction mixture, which was then stirred at 80 °C for 2 h. The reaction mixture was concentrated under reduced pressure, and extracted with diethyl ether. The organic phase was filtered over celite, and the solvent was removed by rotary evaporation in vacuo. Purification of the residue by reduced-pressure distillation gave a transparent oil (3.97 g, 83 %). ^{1}H NMR (500 MHz, $CDCl_3$, TMS): $\delta = 8.22$ (s, 2H), 7.89 (d, $J = 8.1$ Hz, 2H), 7.74 (d, $J = 8.1$ Hz, 2H), 3.92 (q, $J = 7.0$ Hz, 12H), 1.28 ppm (t, $J = 7.0$ Hz, 18H); ^{13}C NMR (125.7 MHz, $CDCl_3$, TMS): $\delta = 136.0$, 133.6, 130.4, 129.6, 127.5, 58.8, 18.2 ppm; HRMS (FAB^+, *m*/*z*): calcd for $C_{22}H_{36}O_6Si_2$ 452.2050 $[M]^+$, found 452.2049.

Synthesis of naphthalene–silica hybrids: 2 M HCl aqueous solution or 6 M NaOH aqueous solution were added to BTENph, C_{18}TMACl, and water with stirring. The reaction mixtures were heated for 24–96 h. Typical synthetic procedures under acidic and basic conditions are described below.

Synthesis under acidic conditions (sample A1): BTENph (0.30 g, 0.66 mmol), C_{18}TMACl (0.40 g, 1.15 mmol), 2 M HCl aqueous solution (15.0 mL), and water (20.0 mL) were stirred at room temperature for 24 h and heated at 95 °C for 24 h. The resultant white precipitate was collected by suction filtration and washed with deionized water. Drying the residue under reduced pressure gave naphthalene–silica hybrid **A1** (denoted as "as-synthesized"). To remove the template surfactant, the as-synthesized sample was dispersed in a mixture of ethanol (20 mL) and 10 M HCl aqueous solution (0.2 mL), and stirred at 60 °C for 12 h. The white powder was collected by suction filtration and washed with ethanol. Drying the residue under reduced pressure gave naphthalene–silica hybrid **A1** without surfactants (denoted as "extracted"). The removal of the surfactant was confirmed by the disappearance of IR absorption bands at $\lambda = 2850$–2960 cm^{-1}, which correspond to C–H stretching modes of alkyl chains.

Synthesis under basic conditions (sample B4): BTENph (0.40 g, 0.88 mmol), C_{18}TMACl (0.35 g, 1.01 mmol), 6 M NaOH aqueous solution (2.0 mL), and water (48.0 mL) was stirred at room temperature for 48 h and heated at 60 °C for 24 h and 95 °C for 24 h. The resultant white precipitate was collected by suction filtration and washed with deionized water. Drying the residue under reduced pressure gave the as-synthesized naphthalene–silica **B4**. Removal of the surfactant by the same method as described for **A1** gave extracted **B4**.

Acknowledgement

We are grateful to Yusuke Akimoto for the TEM observations. We also thank Yoshifumi Maegawa for experimental support in the synthesis of the precursor.

[1] a) A. B. Descalzo, R. Martínez-Máñez, F. Sancenón, K. Hoffmann, K. Rurack, *Angew. Chem.* **2006**, *118*, 6068–6093; *Angew. Chem. Int. Ed.* **2006**, *45*, 5924–5948; b) M. R. Bockstaller, R. A. Mickiewicz, E. L. Thomas, *Adv. Mater.* **2005**, *17*, 1331–1349; c) S. Liu, D. Volkmer, D. G. Kurth, *Pure Appl. Chem.* **2004**, *76*, 1847–1867; d) K. J. C. van Bommel, A. Friggeri, S. Shinkai, *Angew. Chem.* **2003**, *115*, 1010–1030; *Angew. Chem. Int. Ed.* **2003**, *42*, 980–999; e) R. J. P. Corriu, *Angew. Chem.* **2000**, *112*, 1432–1455; *Angew. Chem. Int. Ed.* **2000**, *39*, 1376–1398; f) S. Kitagawa, R. Kitaura, S. Noro, *Angew. Chem.* **2004**, *116*, 2388–2430; *Angew. Chem. Int. Ed.* **2004**, *43*, 2334–2375; g) S. L. James, *Chem. Soc. Rev.* **2003**, *32*, 276–288; h) C. Sanchez, G. J. A. A. Soler-Illia, F. Ribot, T. Lalot, C. R. Mayer, V. Cabuil, *Chem. Mater.* **2001**, *13*, 3061–3083; i) K. J. Shea, D. A. Loy, *Chem. Mater.* **2001**, *13*, 3306–3319.

[2] For mesoporous silica species without organic bridges, see: a) T. Yanagisawa, T. Shimizu, K. Kuroda, C. Kato, *Bull. Chem. Soc. Jpn.* **1990**, *63*, 988–992; b) C. T. Kresge, M. E. Leonowicz, W. J. Roth, J. C. Vartuli, J. S. Beck, *Nature* **1992**, *359*, 710–712; c) J. S. Beck, J. C. Vartuli, W. J. Roth, M. E. Leonowicz, C. T. Kresge, K. D. Schmitt, C. T.-W. Chu, D. H. Olson, E. W. Sheppard, S. B. McCullen, J. B. Higgins, J. L. Schlenker, *J. Am. Chem. Soc.* **1992**, *114*, 10834–10843; d) S. Inagaki, Y. Fukushima, K. Kuroda, *J. Chem. Soc. Chem. Commun.* **1993**, 680–681; e) D. Zhao, J. Feng, Q. Huo, N. Melosh, G. H. Fredrickson, B. F. Chmelka, G. D. Stucky, *Science* **1998**, *279*, 548–552; f) D. Zhao, P. Yang, N. Melosh, J. Feng, B. F. Chmelka, G. D. Stucky, *Adv. Mater.* **1998**, *10*, 1380–1385.

[3] a) W. A. Hunks, G. A. Ozin, *J. Mater. Chem.* **2005**, *15*, 3716–3724; b) F. Hoffmann, M. Cornelius, J. Morell, M. Fröba, *Angew. Chem.* **2006**, *118*, 3290–3328; *Angew. Chem. Int. Ed.* **2006**, *45*, 3216–3251; c) M. P. Kapoor, S. Inagaki, *Bull. Chem. Soc. Jpn.* **2006**, *79*, 1463–1475.

[4] a) S. Inagaki, S. Guan, Y. Fukushima, T. Ohsuna, O. Terasaki, *J. Am. Chem. Soc.* **1999**, *121*, 9611–9614; b) M. P. Kapoor, N. Setoyama, Q. Yang, M. Ohashi, S. Inagaki, *Langmuir* **2005**, *21*, 443–449.

[5] B. J. Melde, B. T. Holland, C. F. Blanford, A. Stein, *Chem. Mater.* **1999**, *11*, 3302–3308.
[6] a) T. Asefa, M. J. MacLachlan, N. Coombs, G. A. Ozin, *Nature* **1999**, *402*, 867–871; b) C. Yoshina-Ishii, T. Asefa, N. Coombs, M. J. MacLachlan, G. A. Ozin, *Chem. Commun.* **1999**, 2539–2540.
[7] J. Alauzun, A. Mehdi, C. Reye, R. J. P. Corriu, *J. Am. Chem. Soc.* **2006**, *128*, 8718–8719.
[8] S. Inagaki, S. Guan, T. Ohsuna, O. Terasaki, *Nature* **2002**, *416*, 304–307.
[9] M. P. Kapoor, Q. Yang, S. Inagaki, *J. Am. Chem. Soc.* **2002**, *124*, 15176–15177.
[10] M. P. Kapoor, Q. Yang, S. Inagaki, *Chem. Mater.* **2004**, *16*, 1209–1213.
[11] A. Sayari, W. Wang, *J. Am. Chem. Soc.* **2005**, *127*, 12194–12195.
[12] M. Cornelius, F. Hoffmann, M. Fröba, *Chem. Mater.* **2005**, *17*, 6674–6678.
[13] Y. Xia, W. Wang, R. Mokaya, *J. Am. Chem. Soc.* **2005**, *127*, 790–798.
[14] a) K. Nakajima, I. Tomita, M. Hara, S. Hayashi, K. Domen, J. N. Kondo, *Adv. Mater.* **2005**, *17*, 1839–1842; b) K. Nakajima, I. Tomita, M. Hara, S. Hayashi, K. Domen, J. N. Kondo, *J. Mater. Chem.* **2005**, *15*, 2362–2368.
[15] M. Ohashi, M. P. Kapoor, S. Inagaki, *Chem. Commun.* **2008**, 841–843.
[16] H. Peng, J. Tang, L. Yang, J. Pang, H. S. Ashbaugh, C. J. Brinker, Z. Yang, Y. Lu, *J. Am. Chem. Soc.* **2006**, *128*, 5304–5305.
[17] K. J. Shea, D. A. Loy, O. Webster, *J. Am. Chem. Soc.* **1992**, *114*, 6700–6710.
[18] R. J. P. Corriu, P. Hesemann, G. F. Lanneau, *Chem. Commun.* **1996**, 1845–1846.
[19] R. Ishii, Y. Shinohara, *J. Mater. Chem.* **2005**, *15*, 551–553.
[20] C.-H. Chen, K.-Y. Liu, S. Sudhakar, T.-S. Lim, W. Fann, C.-P. Hsu, T.-Y. Luh, *J. Phys. Chem. B* **2005**, *109*, 17887–17891.
[21] Y. Goto, N. Mizoshita, O. Ohtani, T. Okada, T. Shimada, T. Tani, S. Inagaki, *Chem. Mater.* **2008**, *20*, 4495–4498.
[22] The formation of the precursory structure of crystal-like walls in naphthalene–silica **B2** was also indicated by fluorescence measurements; see Figure S3 in the Supporting Information.
[23] We also found that molecular-scale periodicities could be induced by the condensation of BTENph in vigorously stirred basic aqueous media without surfactants.
[24] Y. Goto, K. Okamoto, S. Inagaki, *Bull. Chem. Soc. Jpn.* **2005**, *78*, 932–936.
[25] Meso-structured biphenyl–silica hybrids with an amorphous framework were obtained by using the same synthetic procedure with **A1**.
[26] O. Martín, F. Mendicuti, E. Saiz, W. L. Mattice, *J. Polym. Sci. Part B: Polym. Phys.* **1999**, *37*, 253–266.
[27] a) M. Murata, M. Ishikura, M. Nagata, S. Watanabe, Y. Masuda, *Org. Lett.* **2002**, *4*, 1843–1845; b) Y. Maegawa, Y. Goto, S. Inagaki, T. Shimada, *Tetrahedron Lett.* **2006**, *47*, 6957–6960.

Received: June 23, 2008
Revised: September 23, 2008
Published online: November 26, 2008

